Albumin-ruthenium catalyst conjugate for bio-orthogonal uncaging of alloc group

Kimberly S. Taylor,[†] Madison M. McMonagle,[†] Schaelee C. Guy,[†] Ariana M. Human-McKinnon,[†] Shumpei Asamizu,[§] Heidi J. Fletcher,[†] Bradley W. Davis,[†] and Takashi L. Suyama[†]*

[†]Department of Chemistry and Forensic Science, Waynesburg University, 51 W College St, Waynesburg, PA 15370, United States
[§]Engineering Biology Research Center, Kobe University, 1-1 Rokkodai, Nada, Kobe 657-8501, Japan

*Email: tsuyama@waynesburg.edu

Abstract

The employment of antibodies as a targeted drug delivery vehicle has proven successful which is exemplified by the emergence of antibody-drug conjugates (ADCs). However, ADCs are not without their shortcomings. Improvements may be made to the ADC platform by decoupling the cytotoxic drug from the delivery vehicle and conjugating an organometallic catalyst in its place. The resulting protein-metal catalyst conjugate was designed to uncage the masked cytotoxin administered as a separate entity. Macropinocytosis of albumin by cancerous cells suggests the potential of albumin acting as the tumor-targeting delivery vehicle. Herein reported are the first preparation and demonstration of ruthenium catalysts with cyclopentadienyl and quinoline-based ligands conjugated to albumin. The effective uncaging abilities were demonstrated on allyloxy carbamate (alloc)-protected rhodamine 110 and doxorubicin, providing a promising catalytic scaffold for the advancement of selective drug delivery methods in the future.

Introduction

The antibody-drug conjugate (ADC) therapy platform has emerged as a promising class of cancer therapeutics.[1,2] The typical ADC includes a linker covalently connecting a therapeutic to an antibody protein with epitope selectivity for cancer markers (Figure 1). This linker is cleaved in the lysosomal chemical environment upon internalization by a malignant cell, thereby releasing the cytotoxic payload intracellularly. While successful in treating malignancies through this rather eloquent strategy,[1,2] ADCs are not without their own issues.[3,4] Efficacy limitations arising from the confined DAR (drug to antibody ratio),[4,5] off-target release due to the susceptibility of the linker to non-specific cleavage,[4,6] the requirement for timely internalization,[3,7] development of resistance due to the survival of bystander cells,[7,8] lack of penetration into solid tumors,[9] etc, all contribute to the challenges in clinical application of ADCs.

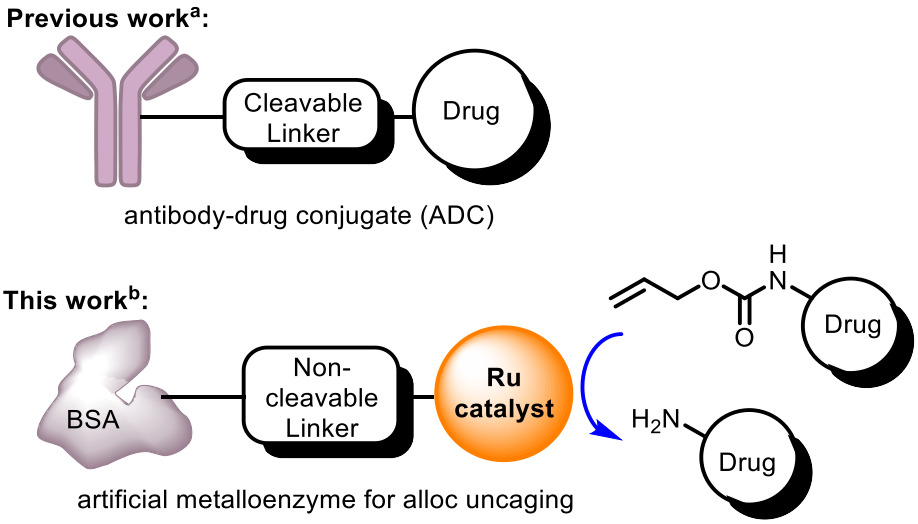

Figure 1. **a** ADC consisting of an antibody linked to a cytotoxic payload, **b** Artificial metalloenzyme consisting of bovine serum albumin conjugated to a ruthenium organometallic catalyst designed to deallylate an alloc-masked drug.

In the meantime, the field of bio-orthogonal chemistry has made advancements, including uncaging reactions catalyzed by transition metals under physiologically relevant conditions, such as the presence of air, water, and thiols.[10–15] Particularly impressive is Meggers and coworkers' long term work with deallylation catalyzed by ruthenium catalysts under such conditions.[13,16,17] For example, the catalyst **1** is readily accessible through a short synthesis from a commercially available material and has a robust reported turnover number (TON) of near 300 for unmasking an alloc-aminocoumarin fluorophore.[13]

Various modes of developing artificial metalloenzymes (ArM) have been reported recently to introduce new-to-nature chemistry.[18–21] The directed evolution strategy was utilized to engineer various ArMs, in which an organometallic catalyst for deallylation was attached to streptavidin via a biotinylated linker.[22] The repertoire of other reactions enabled by ArMs include ring-closing metathesis,[23,24] asymmetric Diels-Alder cycloaddition,[25] cyclopropanation,[26] various redox, hydrolysis, and C-H activation.[19] We hypothesized that conjugation of an organo-ruthenium catalyst to an antibody with affinity for antigens present on malignant cell membrane may enable a novel therapeutic platform wherein caged cytotoxic drugs can be selectively uncaged

at the cancer tissue by the conjugated metal catalyst.[27,28] Herein we refer to this proposed therapy platform as PMC, protein-metal catalyst conjugate.

This proposed platform could overcome a number of issues associated with ADCs. Assuming >1 TON, the amount of the cytotoxic drug released within the tumor microenvironment could exceed that of the corresponding ADC counterpart, which is limited by its DAR.[4,5] Furthermore, stable bio-orthogonal masking groups are not as likely to be prematurely uncaged as some ADCs that have suffered from off-target cleavage of the linker.[4] For example, cathepsin-cleavable dipeptide linkers are susceptible to cathepsin in general circulation and acid-labile hydrazone linkers designed for the low pH of lysosomes are hydrolyzed in human plasma with a t½ = 2 days.[29] In the PMC platform, there is no need for the conjugated moiety to be cleavable. Bystander cells that adapt to downregulate the targeted antigen expressions could still be affected by the extracellularly released drug.[7,8] Therefore, the PMC platform would deter resistance development in the tumor.

Lastly, albumin can be deployed in place of the antibody as a drug delivery vehicle,[30] which would significantly reduce the cost of the therapy (Figure 1). Albumins themselves are preferentially taken up by KRAS-mutated malignant cells through macropinocytosis,[31,32] which can be enhanced further through nutritional manipulation of the tumor via AMP-activated protein kinase (AMPK).[33] Human serum albumin (HSA) has been investigated as a scaffold for ArM due to the anticipated low immunogenicity in humans and glycosylated HSA showed selective targeting properties toward cancer cells.[34,35]

Results and Discussion

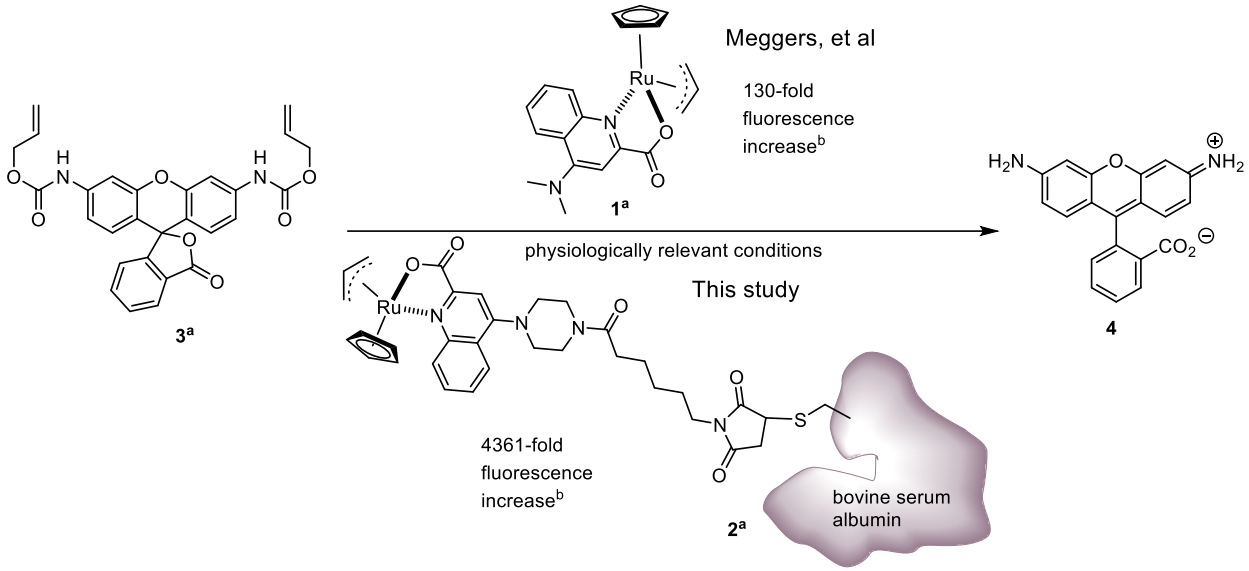

Figure 2. Albumin conjugated to a ruthenium catalyst unmasking bis-alloc-rhodamine 110. **a** Concentrations of **1** and **3** were 20 μM and 100 μM (Meggers et al) and those of **2** and **3** were 30 μM and 150 μM (this study). **b** The fluorescent intensity reached a plateau after 10 minutes for **1**.[13] The catalyst **2** retains catalytic activity after an overnight reaction.

Bovine serum albumin (BSA) possesses a free cysteine residue (Cys34)[36,37] and is convenient for preliminary experiments involving conjugation of maleimide-based linkers[38] compared to antibodies, which would require reduction of the disulfides prior to conjugation.[39] In order to evaluate the catalytic efficiency of the albumin-Ru catalyst conjugate, previously reported alloc$_2$-rhodamine 110 (**3**)[16] was prepared as a model compound to substitute for the caged drug in the proposed PMC platform (Figure 2). In order to ensure that the uncaging activity is due to the ruthenium catalyst that is covalently bonded to the albumin, unconjugated small molecules were eliminated by the use of a 10k molecular weight cut off (MWCO) filter.

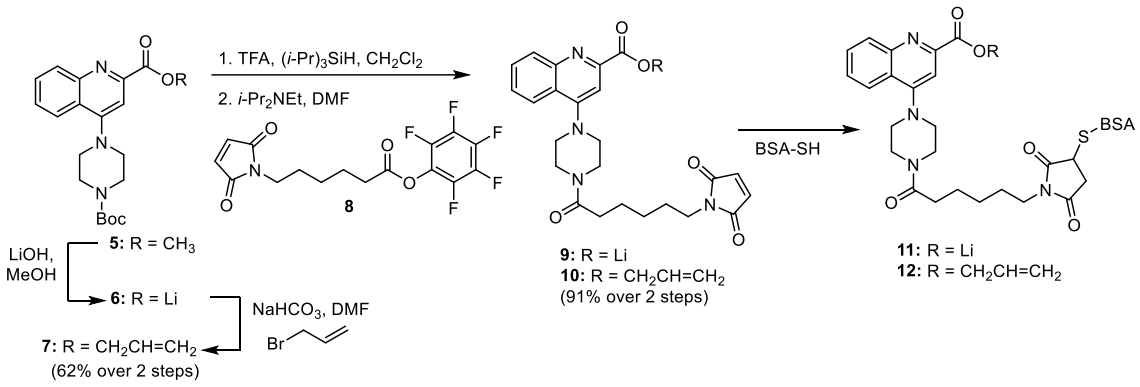

Scheme 1. Synthesis of 2-carboxylatequinoline-based ligands **11** and **12**.

The initial ligand designed for the organo-ruthenium catalyst was the quinolinecarboxylate **9** (Scheme 1). This bidentate ligand was synthesized from a known quinoline ester **5**[40] by deprotection and appending a maleimide linker via a pentafluorophenyl ester.[41,42] However, when **9** was treated with (MeCN)$_3$CpRu, the resulting catalyst was not stable presumably due to ruthenium's affinity toward the maleimide olefin. Therefore, **9** was conjugated to BSA prior to the addition of ruthenium to avoid the side reaction (entry 1, Table 1).[13,16] Upon treatment with (MeCN)$_3$CpRu, this material (**11**) showed deallylation activity against **3**. The incubation time for coordination of the ligand to ruthenium was varied from 15 minutes to 16 hours and the optimum time was determined by measuring the corresponding fluorescence by the uncaged rhodamine 110 (Table-S2). After 16 hours, the catalytic activity significantly diminished, suggesting some instability of the conjugated protein. The uncaging yield as determined by fluorescence peaked with a 2-hour incubation, which can be shortened to 30 minutes without significant loss of performance.

The zwitterion **9** could not be completely purified from the pentafluorophenol byproduct and other impurities even by reverse phase HPLC. In order to ease the purification process for improved catalytic activity, the allyl ester ligand **10** was prepared according to scheme 1.[43] Deconvoluted ESI-LCMS analysis of the conjugated material (**12**) confirmed the expected molecular weight increase for the BSA.[44] The extent of conjugation was estimated to be >50% within the first 30 minutes of incubation at 37 °C based on the mass spectrum (Figure-S3). The relatively low yield of conjugation could be attributed to the cysteine-34 thiol being partially unavailable for conjugation due to oxidation.[45] Pre-treatment of BSA overnight with an excess reducing agent, dithiothreitol (DTT) at pH 6.5, yielded approximately >70% conjugation after 30 minutes of incubation (Figure-S4). Reducing conditions in this pH range apparently do not disrupt the integrity of the disulfide bridges.[45,46] Any longer incubation did not lead to improvements in conjugation as observed by LCMS.

The postulated Ru-catalyzed deallylation mechanism (Scheme-S1)[13] suggests that the rate-determining step (RDS) could be either the uncaging step or the nucleophilic interception of the allylic cation bound to ruthenium. The kinetics of the uncaging step is thought to be largely influenced by the π-donating ability of the metal,[17] which in turn is regulated by the electronic properties of the ligands. Meggers and coworkers showed in their pseudo-Hammet plot that there is an optimal level of electron withdrawing / donating properties of the ligands and a slight change in the electronic properties result in decreased yields.[17] In consideration of the proposed two-step mechanism involving an uncaging step and nucleophilic interception of allylic cation (Scheme-S1),[13] wherein the actual RDS may be elusive, we explored two parallel strategies to improve the uncaging yield; modification of the quinoline ligand to increase its electron-density and introduction of nucleophilic additives for the two proposed steps respectively.

The recent report that an 8-hydroxyquinoline-based Ru catalyst had a higher TON than the quinolinecarboxylate-based catalyst **1**[17] inspired us to pursue the ligand-linker compound **16**, which was prepared according to Scheme 2 starting with the known quinolinecarboxylic acid **13**. Following the literature protocols,[47] the condensation of glycerol with 3-amino-4-hydroxybenzoic acid to construct the quinoline core structure met with much difficulty in isolating the desired product. This issue was remedied by employing diethyl acetal of acrolein as the starting material instead of glycerol (Supplementary Information).

The absence of the ligand virtually abrogated the uncaging ability of the BSA (entry 10, Table 1). In this experiment, BSA was not treated with any ligand, but was treated with CpRu, which was subsequently washed off using a 10k MWCO filter. Therefore, the negligible uncaging yield of 0.5% can be attributed to some amount of CpRu bound to the surface of BSA. Ruthenium is known to bind to albumin fairly well and the Ru-albumin complex is of interest for prevention of metastasis.[48] CpRu by itself, however, does not catalyze deallylation significantly as seen in entry 11 of Table 1.

In our hands, the ArM resulting from **10** performed better than that from **11** in deallylation of **3** (entries 2 and 4, Table 1). In order to evaluate the influence of the albumin conjugation, catalysts not bound to a protein were prepared in an organic solvent from **7** and **15**, and were tested. These protein-free catalysts were subjected to the same reaction conditions, including ligand exchange of Ru occurring in an aqueous solution. A consistent trend was observed that the carboxylate quinoline catalyst Ru-**12** (**2**) provided higher yields than the phenoxide-based catalyst Ru-**17** in contrast to the previous report (entries 2-5, Table 1).[17] When the unbound catalyst derived from **7** was [17] was compared against Ru-12, there was no increase in the yield (entries 2 and 7, Table 1). This implies that the ruthenium coordination and uncaging by the ligand **10** conjugated to BSA are not hindered by the protein.

However, with the 8-hydroxyquinolinate-based ligands, a large discrepancy in the yield between the free (**15**) and conjugated ligands (**16**) was observed, which may indicate that the coordination of ruthenium by **17** is not optimized (entries 4 and 8, Table 1). Hence the equivalency of CpRu and the incubation duration for coordination were increased in an attempt to optimize deallylation by Ru-**17**. While the prolonged incubation time with CpRu did not improve the yield, increasing the equivalence of CpRu for treatment of the conjugated protein prior to washing in the MWCO filter significantly improved the yield from 35% to 56% (entries 4 and 6, Table 1). The relative inefficiency of Ru-**18** indicates that simplification of the quinoline ligand to an aminophenol scaffold may not be achievable.

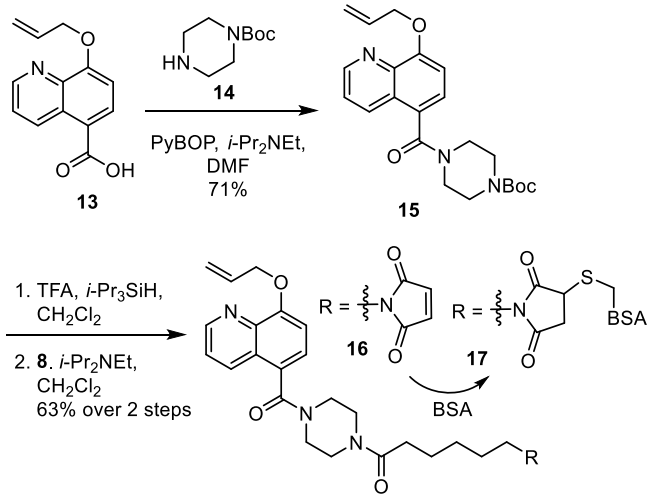

Scheme 2. Synthesis of the 8-hydroxyquinoline-based ligand **17**.

Table 1. Uncaging of alloc$_2$-rhodamine **3** by organoruthenium catalysts[b].

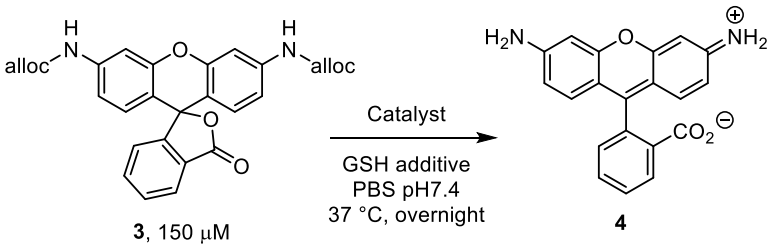

Entry	Ligand	BSA	CpRu	Catalyst[a] (30 μM)	GSH	Yield of **4** (%)
1	**9** (150 μM)	30 μM	300 μM	Ru-**11**	3.5 mM	20
2	**10** (150 μM)	30 μM	150 μM	Ru-**12**	3.5 mM	67
3	**10** (150 μM)	30 μM	150 μM	Ru-**12**	0 mM	22
4	**16** (150 μM)	30 μM	150 μM	Ru-**17**	3.5 mM	35
5	**16** (150 μM)	30 μM	150 μM	Ru-**17**	0 mM	16
6	**16** (150 μM)	30 μM	750 μM	Ru-**17**	3.5 mM	56
7[c]	**7** (30 μM)	0 μM	30 μM	Ru-**7**	3.5 mM	66
8[c]	**15** (30 μM)	0 μM	30 μM	Ru-**15**	3.5 mM	68
9	**18** (30 μM)	0 μM	30 μM	Ru-**18**	3.5 mM	8.2
10[d]	none	30 μM	150 μM	BSA	3.5 mM	0.5
11[e]	none	0 μM	30 μM	CpRu	3.5 mM	0.7
12	none	30 μM	0	BSA	3.5 mM	0.0

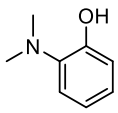

18

a The corresponding ligand was conjugated to BSA in PBS (pH 7.4) at 37 °C for 2 hours. Excess ligand and [CpRu(NCMe)$_3$]PF$_6$ (CpRu) were removed by washing in a 10k MWCO filter tube. **b** Alloc$_2$-rhodamine (**3**, 150 μM) was treated with the resulting BSA-Ru catalyst at 37 °C overnight with agitation. **c** The ligand was treated with CpRu in CH_2Cl_2 and the resulting catalyst was isolated prior to the uncaging reactions. **d** Control experiment where BSA treated

with $[CpRu(CNMe)_3]PF_6$, followed by removal of excess CpRu, was used as the catalyst **e** $[CpRu(CNMe)_3]PF_6$ alone was used as the catalyst.

The observation that the albumin-Ru catalyst conjugate seems to lose its catalytic activity after a long incubation time at 37 °C (Table-S2) prompted investigations into improving the stability of the catalyst by escalating the steric bulk of the cyclopentadienyl ligand. It was hoped that pentamethylcyclopentadienyl ligand (Me_5Cp) would prevent degradation of the catalyst and thereby increasing the TON and perhaps even accelerate the release of allylated nucleophile due to the increased steric hindrance. However, the Me_5Cp ligand diminished the uncaging yield by 13-fold, which is consistent with some earlier reports.[13] Further, we evaluated the stability of the ruthenium catalysts resulting from **12** and **17** by letting their PBS buffer solutions sit at rt in the air for 24 hours and then employing them in the uncaging reaction. The one-day old Ru-**12** catalyst uncaged 3.2% of $alloc_2$-rhodamine **3** while the one-day old Ru-**17** gave 1.7%, implying decomposition of the Ru catalysts over time under physiological conditions, which included 3.5 mM GSH.

Notwithstanding, the 67% yield obtained with the ligand **10** paves a promising path forward for the PMC therapy platform. The concentration of the albumin-Ru catalyst conjugates (30 μM) was 5-fold less than the doubly caged dye (**3**, 150 μM), with the reaction conducted at 37 °C. The achieved uncaging yield surpassing 20% suggests a turnover number (TON) of at least 1, and arguably twice that TON since **3** harbors two allyloxycarbamate groups requiring hydrolysis. The uncaging yield of 67% equates to 101 μM of free rhodamine 110 (**4**) being produced from **3** and 201 μM of uncaged amine groups, indicating a TON of 6.7. While the TONs and % yields reported here appear to be inferior to those reported by Meggers et al for deallylation of alloc-aminocoumarine (270 TON), when comparing the uncaging yield against the same substrate (**3**), Ru-**12** (**2**) performed significantly better than Meggers' unbound catalyst (Figure 2).[13] This quantum yield comparison may represent more accurate evaluation of catalytic utility than the conventional Michaelis value comparison (k_{cat}/K_m).[49]

The kinetic experiments with 2.0 μM catalysts at 20 °C revealed that the catalytic efficiency (k_{cat}/K_m) of the Ru-**12** was 9.6 $M^{-1}s^{-1}$ and that of Ru-**17** was 13 $M^{-1}s^{-1}$. These values were obtained by assuming 100% conjugation of the ligands and 100% loading of Ru. If the actual conjugation and loading efficiencies were less than quantitative, the true catalytic efficiencies would have been higher than reported here. These albumin-based catalysts appear to have strong affinity for the caged rhodamine substrate on par with many enzymes (K_m = $1.4x10^{-6}$ M and $2.3x10^{-6}$ M, respectively), but their actual reaction rates leave room for improvement. In light of the catalytic efficiencies, the higher uncaging yield by Ru-**12** than Ru-**17** may be explained by the relative stability of the quinolinecarboxylate-based catalyst.

Given the sufficiently low K_m, the overall TON could be improved by facilitating the suspected RDS of the nucleophilic interception of the allylic cation (Scheme-S1). Based on Megger's report that the presence of strong nucleophiles such as thiophenol improved the deallylation reaction for some catalysts,[16] we became interested in screening nucleophilic additives that could be relevant under physiological conditions. In our hands, glutathione (GSH) improved the uncaging yield significantly (entries 2 and 3, Table 1), but other nucleophiles such as PhSH, piperazine, and ascorbate slightly decreased the yields. In these uncaging reactions, the concentration of GSH was kept at a commensurate level with that found in tumor tissues (3.5 mM).[50] This is advantageous for targeted delivery due to the tumor microenvironment being normally hypoxic

and thereby promoting a relatively high GSH concentration.[51,52] Meaningful release could be confined to such microenvironments.

Doxorubicin (**20**), which is a cytotoxic drug candidate for the next phase of our PMC platform development due to its well-known pharmacology and the availability of a primary amine in the structure, is administered at a comparable concentration in the human plasma (19~23 μM)[53] to this study. Masked doxorubicin (**19**) is well-tolerated by HeLa cells and a survival rate of almost 80% was noted when treated with 100 μM of **19**.[13] The IC_{50} of doxorubicin (**20**) for HeLa cells is reported to be 2.4 μM, providing an ample therapeutic window.[54] If an antibody is employed in place of albumin, up to 8 molecules of **16** could be conjugated via the reduced cysteine thiols. The demonstrated catalytic efficiency of **12** could then be significantly more than sufficient to provide therapeutically meaningful activation of caged doxorubicin.

To conclude this proof-of-concept study for the PMC platform, we tested the catalysts Ru-**12** and Ru-**17** against alloc-doxorubicin (**19**), which was prepared as reported.[55] The uncaging yield of 27% as determined by ESI-LCMS SIM integration of **20**, equating to 27 μM of **20**, again corroborates the promising nature of our proposal. Interestingly, when **12** was treated with 25 equivalences of CpRu and excess CpRu was removed, the uncaging reaction was apparently complete with no detectable amount of **19** remaining (Figure 3). However, the yield as determined by the LCMS quantification of **20** was still consistently around 20-30%, with no evidence of decomposition, possibly implying that some amount of doxorubicin **20** may be bound to albumin.

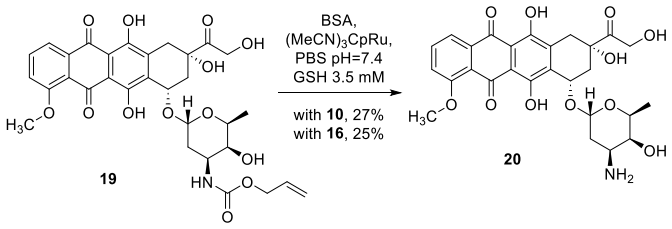

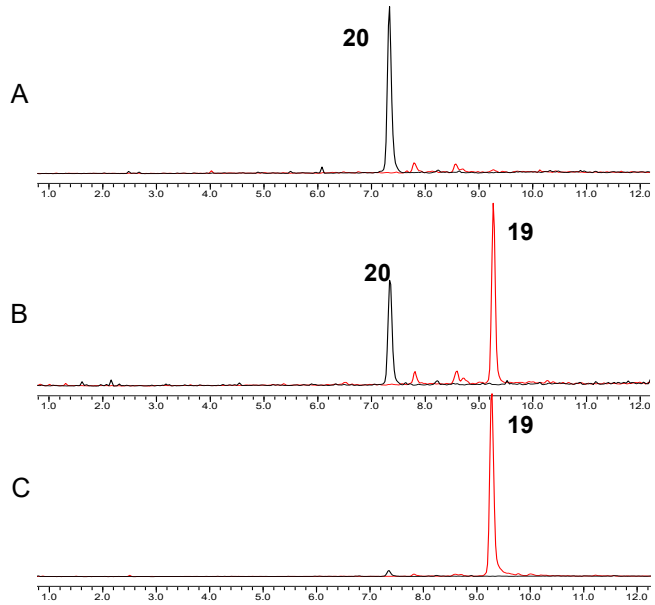

Figure 3. Unmasking of 100 μM alloc-doxorubicin **19** by Ru-**12** or Ru-**17** (30 mol%). A – LCMS chromatogram of uncaging by Ru-**12** (single ion monitoring for 544 m/z for **20** $[M+H]^+$ and 650 m/z for **19** $[M+Na]^+$). B – uncaging by Ru-**17**. C – control experiment lacking a ligand.

Conclusions

In conclusion, we have developed a protocol in which albumin-conjugated ruthenium catalysts efficiently deallylate alloc-protected amines under conditions simulating tumor microenvironments (physiological pH in PBS buffer with elevated GSH level).[16,56] An alternative to the traditional ADC platform was proposed and the successful proof-of-concept experiments described herein will encourage future work utilizing ligands like **10** and **16** conjugated to albumin or antibodies to develop a tissue-selective activation of caged anticancer drugs. While the BSA-Ru catalyst conjugate concentration employed in this study may be considered rather high at 30 μM, the prospect of multiple conjugations of the catalyst per antibody is expected to lower the requisite antibody-Ru conjugate quantity to a level comparable to the micromolar to sub-micromolar plasma concentrations deployed in monoclonal antibody therapies.[57] Moreover, the expected accumulation of the antibody in the targeted tissue would increase the actual concentration of antibody-Ru-conjugate exposed to the caged drug. Alternatively, the target delivery vehicle could remain to be albumin, considering the human plasma concentration of albumin is 530~830 μM,[58] in large excess of the concentrations of BSA-Ru employed in this study (30 μM). Furthermore, the albumin-Ru conjugate could be enriched in the tumor microenvironment through nutritional manipulation of the malignant cells, providing sufficient uncaging selectively.

While this manuscript was being prepared, we became aware of Mao and coworkers' elegant in vivo work with an 8-hydroxyquinolinate-based ruthenium catalyst conjugated to an anti-PD-L1 nanobody uncaging alloc-doxorubicin,[59,60] which substantially validated our PMC hypothesis. However, their catalytic efficiency may not have been as high as reported (Supplementary Information), highlighting the slightly superior in vitro performance of Ru-**12**. Based on our study, the in vivo uncaging efficiency may be enhanced with a quinolinecarboxylate-based ligand, such as **12**. Building on this current work, further optimization of the uncaging reaction and efficacy of the PMC platform are currently under investigation, with results anticipated to be disclosed in due course.

Electronic Supplementary Information

Procedures for synthesizing all new compounds and their characterization, procedures for the uncaging experiments, conjugated albumin's deconvoluted mass spectral data, and precursory uncaging reaction data with ligand **9**, and procedures for kinetic experiments and their data.

Author Contributions

The project was conceptualized by T.L.S., and was developed by T.L.S. and H.J.F. The synthesis of the ligands was carried out by A.M.H-M., K.S.T., M.M.M., and T.L.S. Uncaging experiments were conducted by M.M.M., S.C.G., H.J.F., and T.L.S. Kinetic experiments were

conducted by M.M.M., S.C.G., and T.L.S. and were analyzed by M.M.M., S.C.G., K.S.T., H.J.F., B.W.D., S.A., and T.L.S. The manuscript was written and edited by K.S.T., S.C.G., S.A., H.J.F., and T.L.S, and it was reviewed by all.

Acknowledgements

The financial support from the NSF grant CHE-2102225 is acknowledged. The authors are profoundly grateful for the generous anonymous donation of the JEOL 400 MHz NMR spectrometer, Varioskan Lux spectrophotometer, Beckman centrifuge, and the Büchi Flash system. Some supplies and equipment were provided by the Chemistry and Forensic Science Department at Waynesburg University and the Sigma Xi research grant (G20200315110993198). The Spectroscopy Society of Pittsburgh college equipment grant 2022 is acknowledged for the MS deconvolution software. The HRMS data were skillfully acquired by Dr. Bo Xue at West Virginia University Shared Facilities. Precursory work by Hope Bidelman and adroit assistance in the lab by Hailey Crusenberry are hereby acknowledged. Skillful assistance on the NMR work performed on the ligand **9** by Dr. Novruz Akhmedov is gratefully acknowledged.

Conflict of Interest

The authors disclose that T.L.S. is an active member of the scientific advisory board for Suneco Technologies, Inc and that A.M.H-M. is a current employee for Seek Labs, Inc, but this manuscript is not related to their work at all.

TOC Graphic

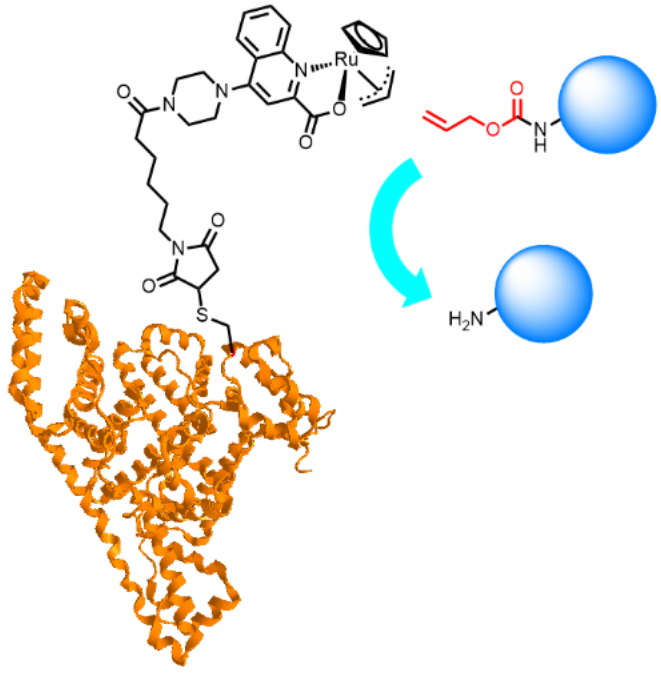

Organo-ruthenium catalyst conjugated to albumin efficiently unmasks alloc group under physiologically relevant conditions.

References

(1) Fu, Z.; Li, S.; Han, S.; Shi, C.; Zhang, Y. Antibody Drug Conjugate: The "Biological Missile" for Targeted Cancer Therapy. *Signal Transduct. Target. Ther.* **2022**, *7* (1), 93. https://doi.org/10.1038/s41392-022-00947-7.

(2) Khongorzul, P.; Ling, C. J.; Khan, F. U.; Ihsan, A. U.; Zhang, J. Antibody–Drug Conjugates: A Comprehensive Review. *Mol. Cancer Res.* **2020**, *18* (1), 3–19. https://doi.org/10.1158/1541-7786.MCR-19-0582.

(3) Dean, A. Q.; Luo, S.; Twomey, J. D.; Zhang, B. Targeting Cancer with Antibody-Drug Conjugates: Promises and Challenges. *mAbs* **2021**, *13* (1), 1951427. https://doi.org/10.1080/19420862.2021.1951427.

(4) Nejadmoghaddam, M.-R.; Minai-Tehrani, A.; Ghahremanzadeh, R.; Mahmoudi, M.; Dinarvand, R.; Zarnani, A.-H. Antibody-Drug Conjugates: Possibilities and Challenges. *Avicenna J. Med. Biotechnol.* **2019**, *11* (1), 3–23.

(5) Sun, X.; Ponte, J. F.; Yoder, N. C.; Laleau, R.; Coccia, J.; Lanieri, L.; Qiu, Q.; Wu, R.; Hong, E.; Bogalhas, M.; Wang, L.; Dong, L.; Setiady, Y.; Maloney, E. K.; Ab, O.; Zhang, X.; Pinkas, J.; Keating, T. A.; Chari, R.; Erickson, H. K.; Lambert, J. M. Effects of Drug–Antibody Ratio on Pharmacokinetics, Biodistribution, Efficacy, and Tolerability of Antibody–Maytansinoid Conjugates. *Bioconjug. Chem.* **2017**, *28* (5), 1371–1381. https://doi.org/10.1021/acs.bioconjchem.7b00062.

(6) Mahalingaiah, P. K.; Ciurlionis, R.; Durbin, K. R.; Yeager, R. L.; Philip, B. K.; Bawa, B.; Mantena, S. R.; Enright, B. P.; Liguori, M. J.; Van Vleet, T. R. Potential Mechanisms of Target-Independent Uptake and Toxicity of Antibody-Drug Conjugates. *Pharmacol. Ther.* **2019**, *200*, 110–125. https://doi.org/10.1016/j.pharmthera.2019.04.008.

(7) Loganzo, F.; Sung, M.; Gerber, H.-P. Mechanisms of Resistance to Antibody–Drug Conjugates. *Mol. Cancer Ther.* **2016**, *15* (12), 2825–2834. https://doi.org/10.1158/1535-7163.MCT-16-0408.

(8) García-Alonso, S.; Ocaña, A.; Pandiella, A. Resistance to Antibody–Drug Conjugates. *Cancer Res.* **2018**, *78* (9), 2159–2165. https://doi.org/10.1158/0008-5472.CAN-17-3671.

(9) Ashman, N.; Bargh, J. D.; Spring, D. R. Non-Internalising Antibody–Drug Conjugates. *Chem. Soc. Rev.* **2022**, *51* (22), 9182–9202. https://doi.org/10.1039/D2CS00446A.

(10) Latocheski, E.; Dal Forno, G. M.; Ferreira, T. M.; Oliveira, B. L.; Bernardes, G. J. L.; Domingos, J. B. Mechanistic Insights into Transition Metal-Mediated Bioorthogonal Uncaging Reactions. *Chem. Soc. Rev.* **2020**, *49* (21), 7710–7729. https://doi.org/10.1039/D0CS00630K.

(11) Liang, T.; Chen, Z.; Li, H.; Gu, Z. Bioorthogonal Catalysis for Biomedical Applications. *Trends Chem.* **2022**, *4* (2), 157–168. https://doi.org/10.1016/j.trechm.2021.11.008.

(12) Liu, Z.; Sun, M.; Zhang, W.; Ren, J.; Qu, X. Target-Specific Bioorthogonal Reactions for Precise Biomedical Applications. *Angew. Chem. Int. Ed.* **2023**, *62* (49), e202308396. https://doi.org/10.1002/anie.202308396.

(13) Völker, T.; Dempwolff, F.; Graumann, P. L.; Meggers, E. Progress towards Bioorthogonal Catalysis with Organometallic Compounds. *Angew. Chem. Int. Ed.* **2014**, *53* (39), 10536–10540. https://doi.org/10.1002/anie.201404547.

(14) Wang, W.; Zhang, X.; Huang, R.; Hirschbiegel, C.-M.; Wang, H.; Ding, Y.; Rotello, V. M. In Situ Activation of Therapeutics through Bioorthogonal Catalysis. *Adv. Drug Deliv. Rev.* **2021**, *176*, 113893. https://doi.org/10.1016/j.addr.2021.113893.
(15) Wu, D.; Yang, K.; Zhang, Z.; Feng, Y.; Rao, L.; Chen, X.; Yu, G. Metal-Free Bioorthogonal Click Chemistry in Cancer Theranostics. *Chem. Soc. Rev.* **2022**, *51* (4), 1336–1376. https://doi.org/10.1039/D1CS00451D.
(16) Streu, C.; Meggers, E. Ruthenium-Induced Allylcarbamate Cleavage in Living Cells. *Angew. Chem.* **2006**, *118* (34), 5773–5776. https://doi.org/10.1002/ange.200601752.
(17) Völker, T.; Meggers, E. Chemical Activation in Blood Serum and Human Cell Culture: Improved Ruthenium Complex for Catalytic Uncaging of Alloc-Protected Amines. *ChemBioChem* **2017**, *18* (12), 1083–1086. https://doi.org/10.1002/cbic.201700168.
(18) Bloomer, B. J.; Clark, D. S.; Hartwig, J. F. Progress, Challenges, and Opportunities with Artificial Metalloenzymes in Biosynthesis. *Biochemistry* **2023**, *62* (2), 221–228. https://doi.org/10.1021/acs.biochem.1c00829.
(19) Davis, H. J.; Ward, T. R. Artificial Metalloenzymes: Challenges and Opportunities. *ACS Cent. Sci.* **2019**, *5* (7), 1120–1136. https://doi.org/10.1021/acscentsci.9b00397.
(20) Liang, A. D.; Serrano-Plana, J.; Peterson, R. L.; Ward, T. R. Artificial Metalloenzymes Based on the Biotin–Streptavidin Technology: Enzymatic Cascades and Directed Evolution. *Acc. Chem. Res.* **2019**, *52* (3), 585–595. https://doi.org/10.1021/acs.accounts.8b00618.
(21) Van Stappen, C.; Deng, Y.; Liu, Y.; Heidari, H.; Wang, J.-X.; Zhou, Y.; Ledray, A. P.; Lu, Y. Designing Artificial Metalloenzymes by Tuning of the Environment beyond the Primary Coordination Sphere. *Chem. Rev.* **2022**, *122* (14), 11974–12045. https://doi.org/10.1021/acs.chemrev.2c00106.
(22) Vornholt, T.; Christoffel, F.; Pellizzoni, M. M.; Panke, S.; Ward, T. R.; Jeschek, M. Systematic Engineering of Artificial Metalloenzymes for New-to-Nature Reactions. *Sci. Adv.* **2021**, *7* (4), eabe4208. https://doi.org/10.1126/sciadv.abe4208.
(23) Fischer, S.; Ward, T. R.; Liang, A. D. Engineering a Metathesis-Catalyzing Artificial Metalloenzyme Based on HaloTag. *ACS Catal.* **2021**, *11* (10), 6343–6347. https://doi.org/10.1021/acscatal.1c01470.
(24) Sauer, D. F.; Gotzen, S.; Okuda, J. Metatheases: Artificial Metalloproteins for Olefin Metathesis. *Org. Biomol. Chem.* **2016**, *14* (39), 9174–9183. https://doi.org/10.1039/C6OB01475E.
(25) Reetz, M. T.; Jiao, N. Copper–Phthalocyanine Conjugates of Serum Albumins as Enantioselective Catalysts in Diels–Alder Reactions. *Angew. Chem. Int. Ed.* **2006**, *45* (15), 2416–2419. https://doi.org/10.1002/anie.200504561.
(26) Huang, J.; Liu, Z.; Bloomer, B. J.; Clark, D. S.; Mukhopadhyay, A.; Keasling, J. D.; Hartwig, J. F. Unnatural Biosynthesis by an Engineered Microorganism with Heterologously Expressed Natural Enzymes and an Artificial Metalloenzyme. *Nat. Chem.* **2021**, *13* (12), 1186–1191. https://doi.org/10.1038/s41557-021-00801-3.
(27) Wang, J.; Wang, X.; Fan, X.; Chen, P. R. Unleashing the Power of Bond Cleavage Chemistry in Living Systems. *ACS Cent. Sci.* **2021**, *7* (6), 929–943. https://doi.org/10.1021/acscentsci.1c00124.
(28) Rossin, R.; van Duijnhoven, S. M. J.; ten Hoeve, W.; Janssen, H. M.; Kleijn, L. H. J.; Hoeben, F. J. M.; Versteegen, R. M.; Robillard, M. S. Triggered Drug Release from an Antibody–Drug Conjugate Using Fast "Click-to-Release" Chemistry in Mice. *Bioconjug. Chem.* **2016**, *27* (7), 1697–1706. https://doi.org/10.1021/acs.bioconjchem.6b00231.
(29) Su, Z.; Xiao, D.; Xie, F.; Liu, L.; Wang, Y.; Fan, S.; Zhou, X.; Li, S. Antibody–Drug Conjugates: Recent Advances in Linker Chemistry. *Acta Pharm. Sin. B* **2021**, *11* (12), 3889–3907. https://doi.org/10.1016/j.apsb.2021.03.042.
(30) Neumann, E.; Frei, E.; Funk, D.; Becker, M. D.; Schrenk, H.-H.; Müller-Ladner, U.; Fiehn, C. Native Albumin for Targeted Drug Delivery. *Expert Opin. Drug Deliv.* **2010**, *7* (8), 915–925. https://doi.org/10.1517/17425247.2010.498474.

(31) Liu, H.; Qian, F. Exploiting Macropinocytosis for Drug Delivery into KRAS Mutant Cancer. *Theranostics* **2022**, *12* (3), 1321–1332. https://doi.org/10.7150/thno.67889.
(32) Quintana, J. M.; Arboleda, D.; Hu, H.; Scott, E.; Luthria, G.; Pai, S.; Parangi, S.; Weissleder, R.; Miller, M. A. Radiation Cleaved Drug-Conjugate Linkers Enable Local Payload Release. *Bioconjug. Chem.* **2022**, *33* (8), 1474–1484. https://doi.org/10.1021/acs.bioconjchem.2c00174.
(33) Li, R.; Ng, T. S. C.; Wang, S. J.; Prytyskach, M.; Rodell, C. B.; Mikula, H.; Kohler, R. H.; Garlin, M. A.; Lauffenburger, D. A.; Parangi, S.; Dinulescu, D. M.; Bardeesy, N.; Weissleder, R.; Miller, M. A. Therapeutically Reprogrammed Nutrient Signalling Enhances Nanoparticulate Albumin Bound Drug Uptake and Efficacy in KRAS-Mutant Cancer. *Nat. Nanotechnol.* **2021**, *16* (7), 830–839. https://doi.org/10.1038/s41565-021-00897-1.
(34) Eda, S.; Nasibullin, I.; Vong, K.; Kudo, N.; Yoshida, M.; Kurbangalieva, A.; Tanaka, K. Biocompatibility and Therapeutic Potential of Glycosylated Albumin Artificial Metalloenzymes. *Nat. Catal.* **2019**, *2* (9), 780–792. https://doi.org/10.1038/s41929-019-0317-4.
(35) Chang, T.-C.; Nasibullin, I.; Muguruma, K.; Kusakari, Y.; Shimoda, T.; Tanaka, K. Evaluation of Acute Toxicity of Cancer-Targeting Albumin-Based Artificial Metalloenzymes. *Bioorg. Med. Chem.* **2022**, *73*, 117005. https://doi.org/10.1016/j.bmc.2022.117005.
(36) Tabata, F.; Wada, Y.; Kawakami, S.; Miyaji, K. Serum Albumin Redox States: More Than Oxidative Stress Biomarker. *Antioxidants* **2021**, *10* (4), 503. https://doi.org/10.3390/antiox10040503.
(37) Wang, R.; Sun, S.; Bekos, E. J.; Bright, F. V. *Dynamics Surrounding Cys-34 in Native, Chemically Denatured, and Silica-Adsorbed Bovine Serum Albumin*. ACS Publications. https://doi.org/10.1021/ac00097a024.
(38) Kratz, F. DOXO-EMCH (INNO-206): The First Albumin-Binding Prodrug of Doxorubicin to Enter Clinical Trials. *Expert Opin. Investig. Drugs* **2007**, *16* (6), 855–866. https://doi.org/10.1517/13543784.16.6.855.
(39) *Antibody-Drug Conjugates: Methods and Protocols*; Tumey, L. N., Ed.; Methods in Molecular Biology; Springer US: New York, NY, 2020; Vol. 2078. https://doi.org/10.1007/978-1-4939-9929-3.
(40) Szponarski, M.; Schwizer, F.; Ward, T. R.; Gademann, K. On-Cell Catalysis by Surface Engineering of Live Cells with an Artificial Metalloenzyme. *Commun. Chem.* **2018**, *1* (1), 84. https://doi.org/10.1038/s42004-018-0087-y.
(41) Prakash, T. P.; Mullick, A. E.; Lee, R. G.; Yu, J.; Yeh, S. T.; Low, A.; Chappell, A. E.; Østergaard, M. E.; Murray, S.; Gaus, H. J.; Swayze, E. E.; Seth, P. P. Fatty Acid Conjugation Enhances Potency of Antisense Oligonucleotides in Muscle. *Nucleic Acids Res.* **2019**, *47* (12), 6029–6044. https://doi.org/10.1093/nar/gkz354.
(42) Park, S.; Lee, M.; Pyo, S.-J.; Shin, I. Carbohydrate Chips for Studying High-Throughput Carbohydrate−Protein Interactions. *J. Am. Chem. Soc.* **2004**, *126* (15), 4812–4819. https://doi.org/10.1021/ja0391661.
(43) Heinisch, T.; Schwizer, F.; Garabedian, B.; Csibra, E.; Jeschek, M.; Vallapurackal, J.; Pinheiro, V. B.; Marlière, P.; Panke, S.; Ward, T. R. E. Coli Surface Display of Streptavidin for Directed Evolution of an Allylic Deallylase. *Chem. Sci.* **2018**, *9* (24), 5383–5388. https://doi.org/10.1039/C8SC00484F.
(44) Adamczyk, M.; Gebler, J. C.; Mattingly, P. G. Characterization of Protein−Hapten Conjugates. 2. Electrospray Mass Spectrometry of Bovine Serum Albumin−Hapten Conjugates. *Bioconjug. Chem.* **1996**, *7* (4), 475–481. https://doi.org/10.1021/bc960035h.
(45) Zhang, Y.; Wilcox, D. E. Thermodynamic and Spectroscopic Study of Cu(II) and Ni(II) Binding to Bovine Serum Albumin. *JBIC J. Biol. Inorg. Chem.* **2002**, *7* (3), 327–337. https://doi.org/10.1007/s00775-001-0302-6.
(46) Katchalski, E.; Benjamin, G. S.; Gross, V. The Availability of the Disulfide Bonds of Human and Bovine Serum Albumin and of Bovine γ-Globulin to Reduction by Thioglycolic Acid. *J. Am. Chem. Soc.* **1957**, *79* (15), 4096–4099. https://doi.org/10.1021/ja01572a034.

(47) Rotili, D.; Altun, M.; Kawamura, A.; Wolf, A.; Fischer, R.; Leung, I. K. H.; Mackeen, M. M.; Tian, Y.; Ratcliffe, P. J.; Mai, A.; Kessler, B. M.; Schofield, C. J. A Photoreactive Small-Molecule Probe for 2-Oxoglutarate Oxygenases. *Chem. Biol.* **2011**, *18* (5), 642–654. https://doi.org/10.1016/j.chembiol.2011.03.007.
(48) Liu, M.; Lim, Z. J.; Gwee, Y. Y.; Levina, A.; Lay, P. A. Characterization of a Ruthenium(III)/NAMI-A Adduct with Bovine Serum Albumin That Exhibits a High Anti-Metastatic Activity. *Angew. Chem. Int. Ed.* **2010**, *49* (9), 1661–1664. https://doi.org/10.1002/anie.200906079.
(49) Eisenthal, R.; Danson, M. J.; Hough, D. W. Catalytic Efficiency and Kcat/KM: A Useful Comparator? *Trends Biotechnol.* **2007**, *25* (6), 247–249. https://doi.org/10.1016/j.tibtech.2007.03.010.
(50) Gamcsik, M. P.; Kasibhatla, M. S.; Teeter, S. D.; Colvin, O. M. Glutathione Levels in Human Tumors. *Biomarkers* **2012**, *17* (8), 671–691. https://doi.org/10.3109/1354750X.2012.715672.
(51) Singleton, D. C.; Macann, A.; Wilson, W. R. Therapeutic Targeting of the Hypoxic Tumour Microenvironment. *Nat. Rev. Clin. Oncol.* **2021**, *18* (12), 751–772. https://doi.org/10.1038/s41571-021-00539-4.
(52) Dabbour, N. M.; Salama, A. M.; Donia, T.; Al-Deeb, R. T.; Abd Elghane, A. M.; Badry, K. H.; Loutfy, S. A. Managing GSH Elevation and Hypoxia to Overcome Resistance of Cancer Therapies Using Functionalized Nanocarriers. *J. Drug Deliv. Sci. Technol.* **2022**, *67*, 103022. https://doi.org/10.1016/j.jddst.2021.103022.
(53) Morris, J.; Dobson, J. Protocols for Administration of Doxorubicin and Cisplatin. In *Small Animal Oncology*; John Wiley & Sons, Ltd, 2001; pp 285–285. https://doi.org/10.1002/9780470690406.app4.
(54) Benyettou, F.; Fahs, H.; Elkharrag, R.; Bilbeisi, R. A.; Asma, B.; Rezgui, R.; Motte, L.; Magzoub, M.; Brandel, J.; Olsen, J.-C.; Piano, F.; Gunsalus, K. C.; Platas-Iglesias, C.; Trabolsi, A. Selective Growth Inhibition of Cancer Cells with Doxorubicin-Loaded CB[7]-Modified Iron-Oxide Nanoparticles. *RSC Adv.* **2017**, *7* (38), 23827–23834. https://doi.org/10.1039/C7RA02693E.
(55) Das, R.; Landis, R. F.; Tonga, G. Y.; Cao-Milán, R.; Luther, D. C.; Rotello, V. M. Control of Intra- versus Extracellular Bioorthogonal Catalysis Using Surface-Engineered Nanozymes. *ACS Nano* **2019**, *13* (1), 229–235. https://doi.org/10.1021/acsnano.8b05370.
(56) Lu, H.; Samanta, D.; Xiang, L.; Zhang, H.; Hu, H.; Chen, I.; Bullen, J. W.; Semenza, G. L. Chemotherapy Triggers HIF-1–Dependent Glutathione Synthesis and Copper Chelation That Induces the Breast Cancer Stem Cell Phenotype. *Proc. Natl. Acad. Sci.* **2015**, *112* (33), E4600–E4609. https://doi.org/10.1073/pnas.1513433112.
(57) Hendrikx, J. J. M. A.; Haanen, J. B. A. G.; Voest, E. E.; Schellens, J. H. M.; Huitema, A. D. R.; Beijnen, J. H. Fixed Dosing of Monoclonal Antibodies in Oncology. *The Oncologist* **2017**, *22* (10), 1212–1221. https://doi.org/10.1634/theoncologist.2017-0167.
(58) Henry, J. B.; McPherson, R. A.; Pincus, M. R. *Henry's Clinical Diagnosis and Management by Laboratory Methods*, 22nd ed.; Elsevier/Saunders: Philadelphia, PA, 2011.
(59) Zhao, Z.; Wang, X.; Wang, J.; Li, Y.; Lin, W.; Lu, K.; Chen, J.; Xia, W.; Mao, Z.-W. A Nanobody–Bioorthogonal Catalyst Conjugate Triggers Spatially Confined Prodrug Activation for Combinational Chemo-Immunotherapy. *J. Med. Chem.* **2023**, *66* (17), 11951–11964. https://doi.org/10.1021/acs.jmedchem.3c00557.
(60) Zhao, Z.; Tao, X.; Xie, Y.; Lai, Q.; Lin, W.; Lu, K.; Wang, J.; Xia, W.; Mao, Z.-W. In Situ Prodrug Activation by an Affibody-Ruthenium Catalyst Hybrid for HER2-Targeted Chemotherapy. *Angew. Chem. Int. Ed.* **2022**, *61* (26), e202202855. https://doi.org/10.1002/anie.202202855.